

3D-QSARs of Herbicidal 2-N-Phenylisoindolin-1-one Analogues as a New Class of Potent Inhibitors of Protox

Min-Gyu Song, Yoon-Jung Lee, and Nack-Do Sung*

Division of Applied Biologies and Chemistry, College of Agriculture and Life Science, Chungnam National University, Daejeon 305-784, Korea. *E-mail: ndsung15@hanmail.net

Received December 3, 2008, Accepted January 28, 2009

3D-QSARs for the inhibition activities against protox by herbicidal 2-N-phenylisoindolin-1-one derivatives were studied quantitatively using CoMFA and CoMSIA methods. The result of the statistical quality of optimized CoMSIA model 2 (FF: r_{ev}^2 : 0.973 & r_{nev}^2 : 0.612) was higher than that of CoMFA model 1 (AF: r_{ev}^2 : 0.414 & r_{nev}^2 : 0.909). Also, the relative contribution of the optimized CoMSIA model 2 showed the steric (24.6%), electrostatic (31.0%), hydrophobic (ClogP, 23.4%) and H-bond acceptor field (21.0%), respectively. From the results of the contour maps, the protox inhibition activities are expected to increase when steric favor and H-bond acceptor favor groups are substituted on R₂ position and positive favor group are substituted on C₂, C₃, and C₅ atom in phenyl ring of R₂ position. And the inhibition activities are expected to increase when hydrophobic favor group is substituted on C₁ and C₃ atom in phenyl ring of R₂ position and Cl atom of R₁ position and hydrophilic favor groups are substituted on C₄ atom in phenyl ring of R₂ position and the terminal group of R₁ position.

Key Words: 3D-QSAR, CoMFA, CoMSIA, 2-N-Phenylisoindolin-1-one analogues, Protox

Introduction

Protox (protoporphyrinogen oxidase: EC 1.3.3.4) inhibitory peroxidizing herbicides¹ have been reported on herbicidal activity according to the modification of alkoxyanilino-substituents in the 2-fluoro-4-chloro-5-alkoxyanilino group.²⁻⁶ Especially, the study for the change of heterocyclic group is actively working.⁷ The common ones of eight types in heterocyclic group are cyclopentane, tetrahydrophthalimide and bicyclic five-membered heterocyclic analogues. Cyclopentane cyclic groups act as a steric factor to fix the position of alicyclic and benzene ring.

For improving herbicidal activity of protox herbicides, SAR (structure-activity relationship) has been studied.⁸ Based on these results, benzoheterocyclic uracil analogues as new protox inhibitors were studied.^{9,10} Recently, the study of herbicidal activity and biochemistry, and also the physiological studies about *N*-(4-chloro-2-fluoro-5-propoxyloxy) phenyl-3,4,5,6-tetrahydrophthalimide analogues have been reported.^{11,12} As part of other trials we reported^{13,14} molecular similarity about not only inhibition activity of *N*-substitution-phenyl-3,4,5,6-tetrahydrophthalimide and *N*-substituted-phenyl-3,4-dimethylmaleimide analogues but also CoMFA analysis. Especially, it is possible to understand the results of CoMFA, CoMSIA and HQSAR,^{15,17} about protox inhibition activity of 1-(5-methyl-3-phenylisoxazolin-5-yl)-methoxy-2-chloro-4-fluorobenzene analogues. Moreover, in the 2-fluoro-4-chloro-5-alkoxy-anilino group, it was found that the change of alkoxyanilino group on C₅ atomic position was more effective than the change of C-phenyl group on herbicidal activity. Also protox inhibition activities are more improved when *ortho* position of C-phenyl group was substituted by the more steric bulky groups.

In this study, the authors have applied CoMFA (comparative molecular field analysis)¹⁸ and CoMSIA (comparative mole-

cular similarity indices analysis)¹⁹ as 3D-QSARs (3 dimensional quantitative structure-activity relationships) method to the herbicidal 2-N-phenylisoindolin-1-one analogues as a new class of potent inhibitors of protox.

Materials and Methods

Protox Inhibition Activity. To measure protox inhibition activity of substrate compounds synthesized by author's published reference,²⁰ the barley and counted chlorophyll contents^{21,22} were selected. Inhibition rate (IN) was calculated by using formula (1).

$$IN(\%) = 100 - \left(\frac{\text{Q'ty chlorophyll}}{\text{Control}} \right) \times 100 \quad (1)$$

From IN (%), the 50% of inhibitory concentration (EC₅₀) was counted. Then formula (2) was inserted and concentration (ppm) was converted into mole concentration (M). Then, the inhibition activity (pI₅₀) was counted from the inversed value of mole concentration with application of -log.

$$Obs. pI_{50} = -\log \left(\frac{EC_{50}(\text{ppm})}{\text{M.Wt.} \times 1,000} \right) \quad (2)$$

Molecular Modeling. All molecular modeling studies, statistical analyses, CoMFA and CoMSIA analyses were performed using SYBYL (Ver. 8.0) program (Tripos Inc.).²³ We carried out CoMFA and CoMSIA analyses to understand quantitatively on the structure-activity relationships (SARs) with 2-N-phenylisoindolin-1-one analogues (Fig. 1),²⁰ as the substrate compounds, and Protox inhibition activity (*Obs. pI₅₀*). Atom partial charge used in the study was applied Gasteiger-Hückel charges^{24,25} and the most stable conformation of the molecules was obtained by simulated annealing method.²⁶ In

this study, CoMFA and CoMSIA models were achieved from training set ($n = 31$) in the data set ($n = 37$) compounds and predictions for the models were evaluated from test set ($n = 6$) compounds. Two different alignment rules in the present study were used: atom based fit (AF) alignment²⁷ and field fit (FF) alignment.²⁸ AF alignment was alignment of the potential energy minimized substrate structures and the results of the alignment of the molecules using AF alignment as shown in Figure 2. On the contour maps, the rate of favor and disfavor contribution (%) was 80% and 20%, respectively.

Calculation of PLS. To conduct CoMFA and CoMSIA model, training set and test set was set arbitrarily. Correlations between 3D-structural feature of aligned compounds on three dimensional spaces and biological activities were calculated by using the PLS (partial least squared) method.²⁹ The cross-validated method was also used to determine the number of optimal component and r^2_{cv} value (or q^2) was represented predictability from the analytical results. The predictive maximum q^2 value and the number of components from the result containing minimum error were selected as optimum number. Cross-validation used leave-one-out (LOO) method,³⁰ which is, excluded compounds from data set by ones. Based on this, correlation coefficient (r^2_{ncv}) was calculated by the non-cross-validation process (scaling: CoMFA standard, column filtering: 2.0 kcal/mol). When correlation coefficient (r^2_{ncv}) was more than 0.90 and predictability (r^2_{cv} or q^2) value was more than 0.50, it is possible to estimate the model has predictability. The component number from the result was used for no-validation and 3D-QSAR model. Also, PRESS (predictive residual sum of the square of the training set) values were calculated by the sum of square deviation between observed values ($Obs.pl_{50}$) of training set and predicted values ($Pred.pl_{50}$).

Results and Discussion

3D-QSAR Models. Observed protox inhibition activity ($Obs.pl_{50}$) of substrate analogues (Fig. 1) has the highest inhibition activity ($Obs.pl_{50} = 6.98$) for compound **29** ($R_1 = 2$ -chloroallyl and $R_2 = 4$ -methoxythiophenyl group). On the other hand, it has the lowest inhibition activity ($Obs.pl_{50} = 4.66$) for compound **20** ($R_1 = 2$ -chloroallyl and $R_2 =$ ethylthio group). According to the change of the substitution group of substrate analogues, CoMFA model and CoMSIA model (Table 1) were calculated from AF and FF alignment. Statistical values of 3D-QSAR models were generated according to the combination condition of range of grid (1.0 ~ 3.0 Å), CoMFA field and CoMSIA field as summarized in Table 2. In CoMFA models, CoMFA 1 model ($r^2_{cv} = 0.414$ and $r^2_{ncv} = 0.909$) from AF alignment condition combined standard field, indicator field and H-bond field was more satisfactory than CoMFA 2 model ($r^2_{cv} = 0.440$ and $r^2_{ncv} = 0.787$) from FF alignment condition. However, the two models were not appropriate because both models could not come to the standard of predictive level (r^2_{cv} or $q^2 > 0.5$).

In CoMSIA models, CoMSIA 2 model ($r^2_{cv} = 0.612$ and $r^2_{ncv} = 0.973$) from FF alignment condition was the more appropriate model with higher correlation than CoMSIA 1

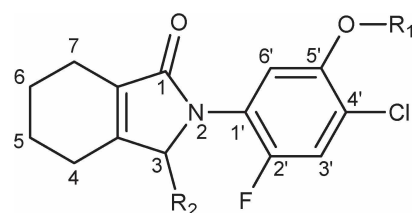


Figure 1. General structure and numbering scheme of 2-N-phenylisoindolin-1-one analogues ($R_1 \sim R_2$).

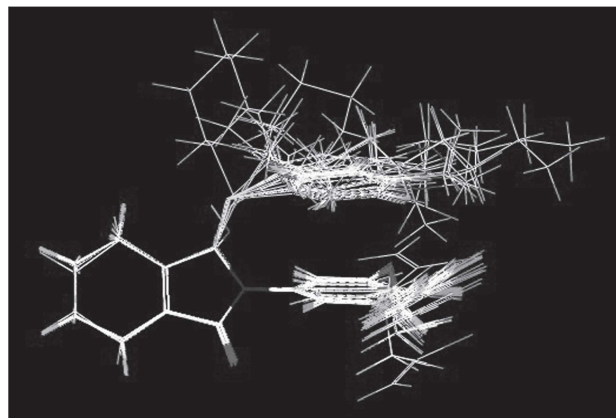


Figure 2. Alignment of the potential energy minimized substrate structures according to a least-squares atom based fit.

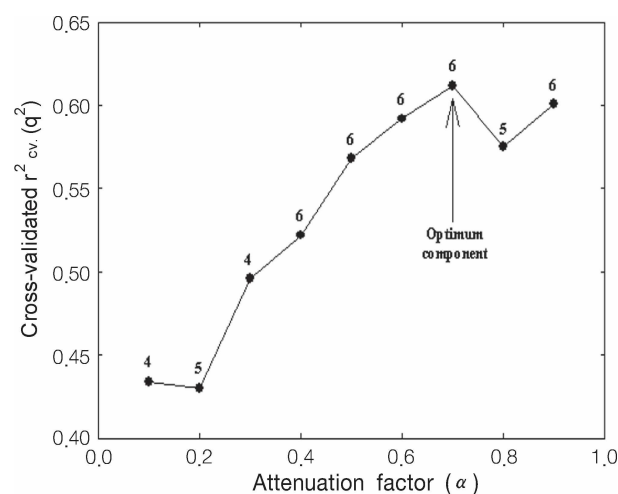


Figure 3. Variation of q^2 upon changing the attenuation factor, α used in the distance dependence between probe atoms and atoms in the molecule with CoMSIA models. (The number on top of the point indicates the optimum number of components).

model ($r^2_{cv} = 0.618$ and $r^2_{ncv} = 0.960$) from AF alignment condition. Therefore, these two models, CoMSIA 1 and 2 models were definitely better models than CoMFA 1 and 2 models statistically. Especially, both CoMSIA 1 and 2 models were appropriate models similarly. The optimized CoMSIA 2 model was the optimized model with a high correlation among four 3D-QSAR models. Observed inhibition activity ($Obs.pl_{50}$) of substrate analogues and predicted inhibition activity ($Pred.pl_{50}$) by CoMSIA 1 and 2 models, and deviation (Dev.) of these two values were summarized in Table 1. The

Table 1. Observed inhibition activity (*Obs.pl₅₀*) against protox and predicted inhibition activity (*Pred.pl₅₀*) by the optimized CoMSIA models using two alignments

No.	Substituents		<i>Obs.pl₅₀</i>	AF		FF ^a	
	R ₁	R ₂		<i>Pred.^b</i>	<i>Dev.^c</i>	<i>Pred.^b</i>	<i>Dev.^c</i>
1	-CH ₂ CCH	(CH ₃)CHS-	5.07	5.04	0.03	4.98	0.09
2	-CH ₂ CCH	(CH ₃) ₃ CS-	5.49	5.39	0.01	5.49	-0.09
3	-CH ₂ CCH	CH ₂ CHCH ₂ S-	5.74	5.73	0.01	5.71	0.03
4	-CH ₂ CCH	CH ₂ (CH ₂) ₂ CH ₂ S-	5.95	6.02	-0.07	6.08	-0.13
5	-CH ₂ CCH	CH ₂ (CH ₂) ₆ CH ₂ S-	6.01	6.07	-0.06	6.19	-0.18
6	-CH ₂ CCH	C ₆ H ₁₀ S-	5.65	5.71	-0.06	5.69	-0.04
7	-CH ₂ CCH	Ph.S-	5.79	6.12	-0.33	5.96	-0.17
9	-CH ₂ CCH	2-CH ₃ -Ph.S-	5.93	6.11	-0.18	5.97	-0.04
10	-CH ₂ CCH	3-CH ₃ -Ph.S-	6.69	6.93	-0.24	6.94	-0.25
11	-CH ₂ CCH	2-Cl-Ph.S-	5.80	5.79	0.01	5.79	0.01
13	-CH ₂ CCH	4-Cl-Ph.S-	6.75	6.35	0.40	6.66	0.09
15	-CH ₂ CCH	4-F-Ph.S-	5.44	5.46	-0.02	5.38	0.06
16	-CH ₂ CCH	3-F-Ph.S-	6.28	6.17	0.11	6.25	0.03
17	-CH ₂ CCH	3-CF ₃ -Ph.S-	5.83	5.91	-0.08	5.83	0.00
18	-CH ₂ CCH	4-CF ₃ -Ph.S-	6.78	6.94	-0.16	6.86	-0.08
19	-CH ₂ CClCH ₂	OH-	5.70	5.73	-0.03	5.60	0.10
20	-CH ₂ CClCH ₂	CH ₃ CH ₂ S-	4.66	4.34	0.32	4.50	0.16
21	-CH ₂ CClCH ₂	(CH ₃) ₂ CHS-	4.91	4.73	0.18	4.91	0.00
23	-CH ₂ CClCH ₂	CH ₂ CHCH ₂ S-	3.96	4.44	-0.48	4.18	-0.22
24	-CH ₂ CClCH ₂	CH ₃ (CH ₂) ₄ CH ₂ S	6.75	6.59	0.16	6.61	0.14
25	-CH ₂ CClCH ₂	CH ₃ (CH ₂) ₆ CH ₂ S	6.78	6.75	0.03	6.79	-0.01
26	-CH ₂ CClCH ₂	C ₆ H ₁₀ S-	5.78	5.96	-0.18	5.81	-0.03
27	-CH ₂ CClCH ₂	2-CH ₃ O-Ph.S-	6.75	6.70	0.05	6.70	0.05
29	-CH ₂ CClCH ₂	4-CH ₃ O-Ph.S-	6.98	6.92	0.06	6.91	0.07
30	-CH ₂ CClCH ₂	2-CH ₃ -Ph.S-	6.07	6.12	-0.05	5.89	0.18
31	-CH ₂ CClCH ₂	3-CH ₃ -Ph.S-	6.88	6.94	-0.06	6.83	0.05
32	-CH ₂ CClCH ₂	2-Cl-Ph.S-	6.68	6.43	0.25	6.61	0.07
33	-CH ₂ CClCH ₂	3-Cl-Ph.S-	6.21	6.00	0.21	6.05	0.16
34	-CH ₂ CClCH ₂	4-Cl-Ph.S-	6.74	6.40	0.34	6.60	0.14
35	-CH ₂ CClCH ₂	2-F-Ph.S-	6.74	6.73	0.01	6.78	-0.04
36	-CH ₂ CClCH ₂	3-F-Ph.S-	5.91	6.18	-0.27	6.17	-0.26

Notes: AF: atom based fit; FF: field fit; ^aoptimized model; ^bpredicted value by the CoMSIA 1 & 2 model; ^cdifference between observed (*Obs.pl₅₀*) values and predicted (*Pred.pl₅₀*) values.

Table 2. Summary of statistical parameters of 3D-QSAR models with two alignments

Model No.	Alignments	PLS Analyses					
		Grid (Å)	NC ^a	r ² _{cv} ^b	r ² _{ncv} ^c	SE _{ncv} ^d	F
CoMFA 1	AF	1.0	2	0.414	0.909	0.246	39.746
CoMFA 2	FF	1.5	3	0.440	0.787	0.353	33.314
CoMSIA 1	AF (α = 0.4)	1.0	6	0.618	0.960	0.163	95.247
CoMSIA 2 ^e	FF (α = 0.7)	1.0	6	0.612	0.973	0.135	141.704

Notes: F: fraction of explained versus unexplained variance; attenuation factor: α; ^anumber of components; ^bcross-validated r²; ^cnon-cross-validated r²; ^dstandard error estimate; ^eoptimized model.

Table 3. Summary of field contribution and PLS results of 3D-QSAR model

Model No.	Field contribution (%)				Training set		Test set	
	S	Hy	E	HA	PRESS	Ave.	PRESS	Ave.
CoMFA 1	76.9	6.60	16.5	-	5.962	0.331	3.547	0.737
CoMFA 2	62.6	24.8	12.6	-	3.327	0.243	3.307	0.697
CoMSIA 1	24.5	27.4	25.8	22.3	1.149	0.145	4.469	0.707
CoMSIA 2 ^e	24.6	23.4	31.0	21.0	0.446	0.096	3.065	0.543

Notes: S: steric field; E: electrostatic field; Hy: hydrophobic field; HA: H-bond acceptor field; ^eoptimized model.

Table 4. Observed protox inhibition activity ($Obs.pl_{50}$) and predicted protox inhibition activity ($Pred.pl_{50}$) by the optimized CoMSIA models for the test set

No.	Substituents		$Obs.pl_{50}$	AF		FF	
	R ₁	R ₂		Pred. ^a	Dev. ^b	Pred. ^a	Dev. ^b
8	-CH ₃ CCH	2-CH ₃ OPh.S-	6.27	5.48	0.79	5.85	0.42
12	-CH ₃ CCH	3-Cl-Ph.S-	5.70	5.78	-0.08	5.66	0.04
14	-CH ₃ CCH	2-F-Ph.S-	5.05	5.49	-0.44	5.74	-0.69
22	-CH ₂ CClCH ₂	(CH ₃) ₃ CS-	6.06	4.60	1.46	4.66	1.40
28	-CH ₂ CClCH ₂	3-CH ₃ O-Ph.S-	5.76	6.96	-1.20	6.43	-0.56
37	-CH ₂ CClCH ₂	3-CF ₃ Ph.S-	5.87	6.14	-0.27	5.91	-0.04

^aThe values were calculated according to the optimized CoMSIA 1 and 2 models in Table 3; ^bdifference between observed activity ($Obs.pl_{50}$) and predicted activity ($Pred.pl_{50}$).

optimized CoMSIA 2 model was combined with steric field, hydrophobic field, electrostatic field and H-bond accept field. From attenuation factor ($\alpha = 0.7$) related to the distance between probe atom and atoms in substrate molecule, cross-validated q^2 (or $r^2_{cv} = 0.62$) value (Fig. 3) was the highest and most optimal component number was 6 in grid 1.0 (Å).

The contribution ratio (%) of distinction fields in 3D-QSAR models, average residual (Ave.) and redictive residual sum of squares (PRESS) of training set (Table 1) and test set compounds (Table 4) were summarized in Table 3. The Ave. and PRESS values of training set and test set with the optimized CoMSIA 2 model were the lowest. From the results, we could understand that CoMSIA 2 model is the most optimized model in all models. The contribution ratio (%) of electrostatic field, steric field, hydrophobicity field and H-bond acceptor field in CoMSIA 2 model was 31.0, 24.6, 23.4 and 21.0%, respectively. Electrostatic field of substrate molecule was greatly contributed to protox inhibition activity. Based on these results, the proportional relationships between observed activities ($Obs.pl_{50}$) related to protox inhibition activity and calculated activities ($Pred.pl_{50}$) by the optimized CoMSIA 2 model were shown in Figure 4. It was expected the statistically appropriate predictibility from this linear

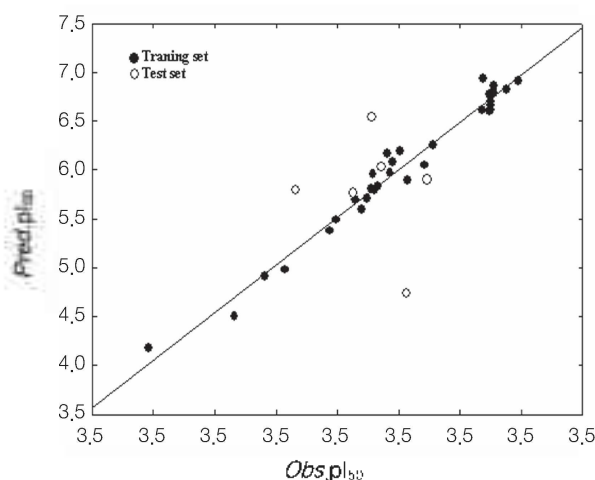


Figure 4. Relationships between observed protox inhibition activities ($Obs.pl_{50}$) and predicted protox inhibition activities ($Pred.pl_{50}$) by the optimized CoMSIA model (Field fit) (For training set: $Pred.pl_{50} = 0.973Obs.pl_{50} - 0.163$, $n = 31$, $s = 0.122$, $F = 1014.78$, $r^2 = 0.972$ & $q^2 = 0.970$).

equation ($Pred.pl_{50} = 0.973Obs.pl_{50} + 0.163$, $n = 31$, $s = 0.122$, $F = 1014.78$, $r^2 = 0.972$ and $q^2 = 0.970$).

Analyses of CoMSIA Contour Maps. The contour maps of the optimized CoMSIA 2 model were represented in Figure 5 and Figure 6. And the most active compound **29** ($R_1 = 2$ -chloroally and $R_2 = 4$ -methoxythiophenyl) is shown in capped sticks. The contour maps in the steric field and the H-bond donor field were represented in Figure 5. The yellow polyhedral regions appeared around R_2 -substituent and its inhibition activity was decreased by bulky substituent sterically. Also, in S-atom region of R_2 -substituents (RS), inhibition

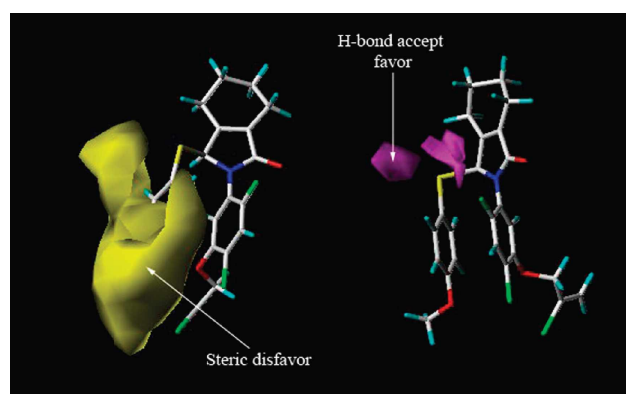


Figure 5. The contour maps of the CoMSIA 2 model for steric field activity (left side) and H-bond accept field (right side) (stdev*coeff). The most active compound (**29**) is shown in capped sticks.

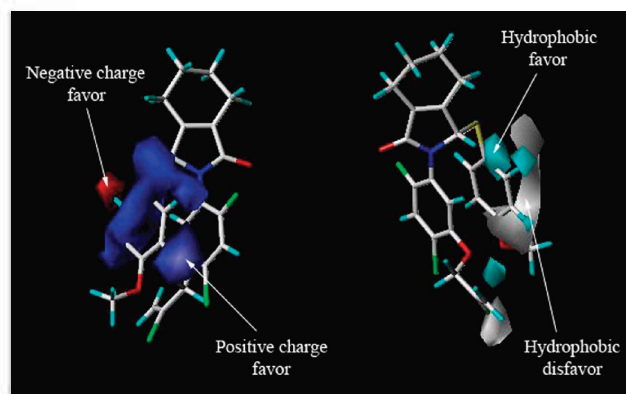


Figure 6. The contour maps of the CoMSIA 2 model for electrostatic field (left side) and hydrophobic field (right side) (stdev*coeff). The most active compound (**29**) is shown in capped sticks.

activity was implied increase by the substituent (purple color) favored H-bond acceptor field. The contour maps in the electrostatic field and the hydrophobic field were represented in Figure 6. According to the results of the contour maps in the electrostatic field, the blue polyhedra favored positive charge were strongly expressed in two positions: where in combination of R₂-substituent and its template, where in C₂, C₃ and C₅ carbon atoms of phenyl ring. The inhibition activity was presumed increase by the positive charge substituent in the blue polyhedra and by negative charge substituent (red color polyhedra) in C₆ carbon atom. According to the results of the contour maps in the hydrophobic field on the right side, the protox inhibition activity was predicted increase by not only the hydrophobic substituent (silver polyhedral region) in C₁ atom of S-phenyl ring and C₅ of carbon atom but also the hydrophilic substituent (cyan polyhedral region) in C₄ carbon atom of S-phenyl ring. From the analyses results of these optimized CoMSIA 2 model, the structural distinctions that contribute to the herbicidal activity with inhibition of protox were obtained.

Conclusion

The CoMSIA 2 model is the most optimized ($r_{cv}^2 = 0.612$ & $r_{ncv}^2 = 0.973$) model among four 3D-QSAR models from two alignment conditions (AF and FF) to explain the protox inhibition activity of herbicidal substrate molecules. According to the distinction field, the protox inhibition activities depend on the electrostatic field (31.0%). From the contour maps, when steric factor is small in R₂-substituent position, inhibition activity is increased. The substituent preferred to the positive charge at C₂, C₃ and C₅ carbon atom in phenyl ring, and the substituent preferred to the negative charge at C₆ carbon atom making inhibition activity increase. Also the protox inhibition activity was predicted increase by not only the hydrophobic substituent at C₁ and C₃ carbon atom of R₂-substituent in S-phenyl ring but also the hydrophilic substituent at C₄ atom position of R₁-substituent, C₄ carbon atom and in the end of R₁-substituent.

Acknowledgments. This work was supported by a grant (No. R11-2002-100-00503) from Engineering Research Center (ERC) Program of the Korea Science and Engineering Foundation (KOSEF).

References

- Boger, P.; Wakabayashi, K. In *Peroxidizing Herbicides*; Springer-Verlag: Berlin, Heidelberg, Germany, 1999.
- Fujita, T. In *Agrochemical Discovery; Insect, Weed, and Fungal Control: Similarities in Bioanalogous Structural Transformation Patterns*. ACS Symposium Series; Baker, D. R.; Umetsu, N. K., Eds.; American Chemical Society: Washington DC, 2002; Ch. 15, No. 774.
- Hiraki, M.; Ohki, S.; Sato, Y.; Jablonkai, I.; Boger, P.; Wakabayashi, K. *Pesticide Biochemistry and Physiology* **2001**, *70*, 159.
- Ishida, S.; Miller-Sulger, R.; Kohno, H.; Boger, P.; Wakabayashi, K. *J. Pestic. Sci.* **2000**, *25*, 18.
- Iida, T.; Uchida, A.; Uruguchi, R.; Sato, Y.; Boger, P.; Wakabayashi, K. *J. Pestic. Sci.* **1997**, *22*, 303.
- Ishida, S.; Hirai, K.; Kohno, H.; Sato, Y.; Kubo, H.; Boger, P.; Wakabayashi, K. *J. Pestic. Sci.* **1997**, *22*, 299.
- Pallett, K. E. *Proceeding of Brighton Crop Protection Conference-Weeds*; 1997; p 575.
- Theodoridis, G. *Pestic. Sci.* **1997**, *50*, 283.
- Theodoridis, G.; Bahr, J. T.; Hotzman, F. W.; Sehgel, S.; Suarez, D. P. *Crop Prot.* **2000**, *19*, 533.
- Hiraki, M.; Ohki, S.; Sato, Y.; Jablonkai, I.; Boger, P.; Wakabayashi, K. *Pesticide Biochemistry and Physiology* **2001**, *70*, 159.
- Watanabe, N.; Takayama, S.; Yoshida, S.; Isogai, A.; Che, F. S. *Biosci. Biotechnol. Biochem.* **2002**, *66*, 1799.
- Dayan, F. E.; Duke, S. O.; Reddy, K. N.; Hamper, B. C.; Leschinsky, K. L. *J. Agric. Food Chem.* **1997**, *45*, 967.
- Sung, N. D.; Ock, H. S.; Chung, H. J.; Song, J. H.; Lee, Y. G. *Kor. J. Pest. Sci.* **2003**, *7*, 75.
- Sung, N. D.; Ock, H. S.; Chung, H. J.; Song, J. H. *Kor. J. Pest. Sci.* **2003**, *7*, 100.
- Sung, N. D.; Song, J. H.; Yang, S. Y.; Park, K. Y. *Kor. J. Pest. Sci.* **2004**, *8*, 151.
- Sung, N. D.; Song, J. H.; Park, K. Y. *J. Kor. Soc. Appl. Biol. Chem.* **2004**, *47*, 351.
- Sung, N. D.; Song, J. H.; Park, K. Y. *J. Kor. Soc. Appl. Biol. Chem.* **2004**, *47*, 414.
- Cramer, R. D., III; Patterson, D. E.; Bunce, J. E. *J. Am. Chem. Soc.* **1988**, *110*, 5959.
- Klebe, G.; Abraham, U.; Mietzner, T. *J. Med. Chem.* **1994**, *37*, 4130.
- Cho, Y. G.; Soung, M. G.; Sung, N. D. 2007 *International Symposium and Annual Meeting of the KSABC*, Gyeongju, Korea, 2007.
- Johan, B. *Photochem and Photobiol.* **1963**, *2*, 241.
- Hiscox, J. D.; Israelstan, G. F. *Can. J. Bot.* **1978**, *57*, 1332.
- Tripos, Sybyl. *Molecular Modeling and QSAR Software on CD-Rom* (Ver. 7.3); Tripos Associates, Inc.: Suite 303, St. Louis, MO.
- Purcell, W. P.; Singer, J. A. *J. Chem. Eng. Data* **1967**, *122*, 235.
- Gasteiger, J.; Marsili, M. *Tetrahedron* **1980**, *36*, 3219.
- Kerr, R. *Biophys. J.* **1964**, *67*, 1501.
- Marshall, G. R.; Barry, C. D.; Bosshard, H. E.; Dammkoehler, R. A.; Dunn, D. A. In *Computer-assisted Drug Design: The Conformational Parameter in Drug Design; Active Analog Approach*; Olsen, E. C.; Christoffersen, R. E., Eds.; American Chemical Society: Washington, D.C., 1979; p 205.
- Clark, M.; Cramer III, R. D.; Jones, D. M.; Patterson, D. E.; Simeroth, P. E. *Tetrahedron Comput. Methodol.* **1990**, *3*, 47.
- Stahle, L.; Wold, S. *Progr. Med. Chem.* **1988**, *25*, 292.
- Cramer, R. D.; Bunce, J. D.; Patterson, D. E. *Quant. Struct. Act. Relat.* **1988**, *7*, 18.